

# Glycosylation of prions and its effects on protein conformation relevant to amino acid mutations

Nicky K.C. Wong,\* David V. Renouf,\* Sylvain Lehmann,† and Elizabeth F. Hounsell\*

\*School of Biological & Chemical Sciences, Birkbeck, University of London, London, United Kingdom  
†IGH du CNRS, Montpellier, France

The three-dimensional coordinates from a nuclear magnetic resonance (NMR)-averaged structure containing residues 121–226 of mouse prion were used as the starting geometry for MD of prion either with or without glycan in both mutant and wild-type forms. The following mutants were studied: Asp-178 to Asn, Thr-183 to Ala, Phe-198 to Ser, Glu-200 to Lys, and Gln-217 to Arg. NMR data vs structural models were compared to observe any major differences. Simulations of the change in protein structure with and without glycan were performed, as they cannot be tested by NMR analysis. Several mutants were expressed and analyzed for altered glycosylation and the results interpreted in terms of molecular modeling. N-linked glycosylation is likely to play an important role in prion biology as shown by visualization of glycoprotein conformation.

**Keywords:** prion protein, glycosylation, mutant, molecular dynamics, modeling

**Abbreviations:** PrP, prion protein; PrP<sup>C</sup>, normal cellular isoform of prion protein; PrP<sup>Sc</sup>, pathogenic scrapie isoform of prion protein; mPrP, mouse PrP; mPrP (124–231), fragment of mPrP; mPrP (23–231), complete polypeptide of mature mPrP; hPrP, human PrP; MD, molecular dynamics; GlcNAc, N-acetyl-D-glucosamine; Fuc, fucose; NMR, nuclear magnetic resonance; PDB, protein data bank; PDB1ag2, the code number of the atom coordinates of the refined mean structure of mPrP (121–231), which has been deposited in the PDB; TSE, transmissible spongiform encephalopathy.

Color Plates for this article are on pages 163–165.

Corresponding author: Nicky K.C. Wong, School of Biological & Chemical Sciences, Birkbeck, University of London, Gordon House, 29 Gordon Square, London, WC1H 0PP, United Kingdom. Tel.: +44 207 679 4642; fax: +44 207 380 7464.

E-mail address: n.wong@sbc.bbk.ac.uk (N.K.C. Wong)

## INTRODUCTION

Prions are a novel class of pathogens that have been proposed to be the cause of transmissible spongiform encephalopathies (TSEs).<sup>1</sup> TSEs are fatal neurodegenerative disorders that include kuru, Creutzfeldt-Jakob disease (CJD), fatal familial insomnia (FFI), and Gerstmann-Strässler-Scheinker (GSS) syndrome in humans, scrapie in sheep, and bovine spongiform encephalopathy (BSE). The cellular form of mammalian PrP (PrP<sup>C</sup>) consists of a single polypeptide chain containing two N-linked glycosylation sites<sup>2</sup> and is attached to the cell surface by a glycosyl-phosphatidyl-inositol (GPI) anchor at its carboxyl terminus.<sup>3</sup> Pathological PrP (PrP<sup>Sc</sup>) is thought to be a conformationally altered isoform of PrP<sup>C</sup>, although both PrP isoforms contain the same amino acid sequence<sup>3</sup> and similar covalent modifications. The molecular mechanism by which PrP<sup>C</sup> is converted into PrP<sup>Sc</sup> is unknown. However, it is likely that it involves the transition of  $\alpha$ -helices to  $\beta$ -sheets in certain regions of the polypeptide chain.<sup>4</sup> Studies have suggested that oligosaccharide chains may modulate the efficiency of the conversion process and may serve as specific molecular markers in various prion strains.<sup>5–8</sup>

Riek et al.<sup>9–11</sup> used a refined NMR data set of mPrP (121–231) to predict the likely structural and functional consequences of amino acid substitution in human PrP (hPrP) that are associated with inherited familial TSEs.<sup>12</sup> These mutations are all located within, or sequentially adjacent to, helices 2 and 3 of the PrP molecule close to the glycosylation sites. However, in the papers published by Riek et al.,<sup>9–11</sup> the expressed PrP would not be glycosylated. Therefore, we simulated the glycosylation of PrP by molecular dynamics (MD) and analyzed the resultant model in the context of the mutants discussed by Riek et al.<sup>11</sup> and our studies here on SDS-PAGE analysis of altered glycosylation in cell expression. Correlations between the molecular structure of the prion mutants and their role in TSE pathology have been described on the basis of structural predictions.<sup>13</sup> For example, one of the mutations studied here, Asp-178-Asn, when present with homozygous Met polymorphism at 129, results in FFI and when present

with homozygous Val-129 results in familial CJD.<sup>14</sup> The Met/Val polymorphism at 129 does not cause disease in the presence of wild-type Asp-178, but Met or Val homozygosity appears to predispose to sporadic prion disease in Caucasians<sup>15</sup> but not in Asians.<sup>16</sup> Studies by Cohen et al.<sup>4</sup> suggest that inherited TSEs might be related to destabilization of the three-dimensional structure of PrP<sup>C</sup> and lead to formation of other conformational states. Moreover, point mutations at these sites may influence PrP ligand-binding properties.<sup>17</sup> To study this in the context of prion glycosylation, we show here that, using molecular modeling and the AMBER force field, we can recreate the predictions of Riek et al.<sup>11</sup> regarding the mutants and show the effects of glycosylation on protein conformation, which we correlated with the altered glycosylation patterns shown by SDS-PAGE analysis. Using MD, experimental models were made to predict protein stability due to changes in internal H-bond and hydrophobic interactions of mutants. In addition, modeling of the mutant Glu-200-Lys provided more information than the NMR experiments in explaining the cell expression data of altered glycosylation.

## MATERIALS AND METHODS

### Molecular Modeling

The three-dimensional coordinates from a NMR-averaged structure (PDB1ag2) containing residues 124-226 of *mPrP*<sup>C</sup> were used.<sup>11</sup> Structures were constructed (InsightII 97.0, MSI)

containing either a representative biantennary, bisected, core and Le<sup>x</sup> fucosylated, nonsialylated undecasaccharide<sup>18</sup> or a trisaccharide composed of GlcNAc $\beta$ 1-4(Fuc $\alpha$ 1-6)GlcNAc $\beta$ 1- at two N-linked glycosylation sites (positions Asn-181 and Asn-197). The glycan was constructed for use with the AMBER force field as previously described,<sup>19</sup> with all dihedral angles set to minimum energy conformations.<sup>20,21</sup> The distant dielectric constant was set at 4 × r to allow for variations in simulated solvent at the protein surface and the more hydrophobic core protein residues. The structures were relaxed using a stepwise minimization procedure (Discover MSI). For each mutant, residues within 10 Å were determined and used to define a subset of residues present in the environment local to the mutation. These subsets were different for each mutant and are detailed in Figure 1. The minimization used conjugate gradients to a maximum derivative of 0.001 kcal/A over three steps. In the first step, side-chain atoms of the subset were allowed to minimize while all other atoms were fixed. In the second step, all atoms of the subset plus the side-chain atoms of all other residues were minimized. In the third step, all atoms were free to move. In all steps, the atoms of the glycan were free to move. MD runs of 1 ps equilibration followed by 50 ps at 300 K with the atoms fixed as in the last minimization step, followed by another 50 ps with all atoms free to move. Coordinates were saved every 0.5 ps. Each mutant was run with and without glycan attached. For the controls of each mutant, the

124	131	141	151	161	171
GLGGYML	GSAMSRPMIH	FGNDWEDRYYY	RENMYRYPNQ	VYYRPVDQYS	NQNNFVHDCV
GLGGYML	GSAMSRPMIH	FGNDWEDRYYY	RENMYRYPNQ	VYYRPVDQYS	NQNNFVHDCV
GLGGYML	GSAMSRPMIH	FGNDWEDRYYY	RENMYRYPNQ	VYYRPVDQYS	NQNNFVHDCV
GLGGYML	GSAMSREMIH	FGNDWEDRYYY	RENMYRYPNQ	VYYRPVDQYS	NQNNFVHDCV
GLGGYML	GSAMSRPMIH	FGNDWEDRYYY	RENMYRYPNQ	VYYRPVDQYS	NQNNFVHDCV
GLGGYML	GSAMSRPMIH	FGNDWEDRYYY	RENMYRYPNQ	VYYRPVDQYS	NQNNFVHDCV
bbb	b	aaaaaaaa	aaaa	bbbb	aa s
S					
181	191	201	211	221	Wild-type
NITIKQHTVT	TTTKGENFTE	TDVKMMERVV	EQMCVTQYQK	ESQAYY	
NITIKQHTVT	TTTKGENFTK	TDVKMMERVV	EQMCVTQYQK	ESQAYY	Phe-200-Lys
NIAIKQHTVT	TTTKGENFTE	TDVKMMERVV	EQMCVTQYQK	ESQAYY	Thr-183-Ala
NITIKQHTVT	TTTKGENFTE	TDVKMMERVV	EQMCVTTRYQK	ESQAYY	Gln-217-Arg
NITIKQHTVT	TTTKGENFTE	TDVKMMERVV	EQMCVTQYQK	ESQAYY	Asp-178-Asn
NITIKQHTVT	TTTKGENSTE	TDVKMMERVV	EQMCVTQYQK	ESQAYY	Phe-198-Ser
aaaaaaaaaaa	aaa	a	aaaaaaaaaaa	aaaaaaa	

Figure 1. Sequence of mutants. For each amino acid mutation (white on black box), residues within 10 Å (enclosed by boxes) defined a subset of residues present in the environment local to the mutation, which were allowed freedom of movement during the simulation.

wild-type with and without glycan attached were run under the same protocols. Once minimization and MD was completed for each mutant and wild-type, an average structure from the last 10 ps of the final MD was generated, minimized, and the LIGPLOT program used<sup>22</sup> to assess H-bonding of residues and hydrophobic contacts of interest.

### Chinese Hamster Ovary Cell Cultures

Construction of cDNAs encoding wild-type and mutant *mPrP* that are derived from the *prnp-a* allele, as well as generation and cultures of stably transfected lines of Chinese hamster ovary (CHO) cells expressing wild-type, and mutated Asp-178-Asn and Glu-200-Lys *mPrP* have been described previously.<sup>23–25</sup> CHO cells were grown in MEM- $\alpha$  containing 7.5% fetal calf serum (FCS), 300  $\mu$ g/mL geneticin and penicillin/streptomycin in an atmosphere of 5% CO<sub>2</sub>/95% air. Confluent cultures of CHO cells were labeled for 4 hours in methionine-free MEM containing Tran<sup>35</sup>S-label (250–500  $\mu$ Ci/mL) and nonessential amino acids. Cells were lysed in a buffer that contained 150 mM NaCl, 50 mM TRIS (pH 7.5), 0.5% Triton X-100, and 0.5% sodium deoxycholate, and supplemented with protease inhibitors (pepstatin and leupeptin 1  $\mu$ g/mL; PMSF 0.5 mM; EDTA 2 mM). Samples from metabolically labeled cells were immunoprecipitated using the rabbit polyclonal antibody P45-66, raised against a synthetic peptide encompassing *mPrP* residues 45–66, as described previously.<sup>25</sup> Where indicated, cell lysates were treated before immunoprecipitation with 0.01 U/mL of peptide-*N*-glycosidase F (PNGase F) for 16 hours at 37°C. The immunoprecipitates were analyzed by SDS-PAGE.

## RESULTS

MD studies of the glycosylated wild-type suggested that there was little influence of the distal parts of the oligosaccharides or the protein; therefore, a trisaccharide composed of GlcNAc $\beta$ 1-4(Fuc $\alpha$ 1-6)GlcNAc $\beta$ 1- on residues Asn-181 and Asn-197 (Color Plate 1) was used in the MD simulations. The following mutants were studied: Asp-178 to Asn, Thr-183 to Ala, Phe-198 to Ser, Glu-200 to Lys, and Gln-217 to Arg. The glycan of the GPI was removed for the mutant studies, and this will be the subject of a future study on the GPI-lipid membrane. Each mutant was compared with the original PBD1ag2 file and, after minimization defined as wild-type with or without glycan, was analyzed using the LIGPLOT program to define the hydrophobic and hydrogen-bond contacts. The mutants discussed below range either side and between the two glycosylation sites shown in Color Plate 1.

### Effects of Single Amino Acid Mutations on Prion Conformation

**Phe-198-Ser** Residue Phe-198 is inward facing on an extended loop between two helices. In the absence of glycosylation, this mutation to Ser was thought<sup>11</sup> to disrupt a “hydrophobic core” of the molecule and leave a cavity for inclusion of water. MD simulations of the nonglycosylated mutant (Table 1) resulted in abolition of hydrophobic interactions around the mutant residue, which is in agreement with results of previous NMR studies.<sup>11</sup> For the glycosylated mutant (Table 1), an additional hydrophobic interaction between residue Ser-198

and Val-203 was observed, and the Fuc of the glycosylation came into close proximity to the cavity space (Color Plate 2A). Moreover, a decrease of  $\alpha$ -helix content was observed in comparison to the wild-type with and without glycan. For the nonglycosylated wild-type, one H-bond contact was observed (Phe-198 N-O Glu-196). With respect to hydrophobic interactions, for both wild-type with and without glycan, numerous residues are surrounding the Phe aromatic ring, as in the PDB1ag2 data. Visualization of the glycosylation in the wild-type for Phe-198-Ser mutant shows that the glycan sits on top of the protein surface, without major effects on the protein conformation (Color Plate 2B). Residues involved in hydrophobic interactions (gray) surround the Phe-198 aromatic ring (green) at various positions within the hydrophobic core, thus stabilizing the structure. In comparison, replacement of the Phe-198 residue with Ser results in significant displacement of the glycan at position Asn-197 due to collapse of the hydrophobic core (Color Plate 2A). This is shown by the absence of hydrophobic residues interacting with the mutant residue within this region. Thus, the Fuc residue (white) is shown to be replacing the water molecules inside the cavity, whereas the two GlcNAc residues (yellow) are contacting the local surface structure.

Closer examination of the mutant (Color Plate 2C) shows that the glycan at Asn-197 is surrounded by a variety of independently formed H-bond and hydrophobic interactions (gray). Residues involved in H-bonding to the glycan (mainly to the Fuc residue) include Thr-188, Glu-196, Thr-199, Thr-192, and Val-189, whereas residues involved in hydrophobic interaction include Gly-195 and Lys-194. For comparison, in the wild-type (Color Plate 2D), the influence of glycan on the protein structure is relatively weak. Only one residue is involved in H-bonding (Thr-192) and one in hydrophobic interaction (Thr-188) to the glycan. Residue Thr-192 is shown to interact with GlcNAc, whereas in the mutant, this residue is interacting with Fuc.

A longer MD run of the mutant was carried out to visualize the effect of glycan with respect to protein conformation. An average structure of the last 250 of 5000 ps of the mutant was minimized. This additional 5000 ps MD on the protein changes the position of the glycan at Asn-197 (not shown) to give H-bond contacts of GlcNAc (linked to Asn) to Val-189, Thr-188, and Lys-185 and of Fuc to Ser-198 and Glu-200.

**Glu-200-Lys** Riek et al.<sup>11</sup> could only predict minor changes in protein conformation based on the Glu-200 to Lys mutation. Our results by SDS-PAGE show that the glycosylation of this mutant is greatly reduced in comparison to the wild-type (Figure 2) due to the altered protein conformation. Similar reduction in glycosylation was found in familial CJD patients with the Glu-200-Lys point mutation.<sup>26</sup> Based on LIGPLOT results (Table 1), the mutants with and without glycan indicate that there are no major changes with respect to H-bonding between the wild-types and the original PDB1ag2 data, which is in agreement with the NMR data on nonglycosylated prion. However, in the glycosylated mutant, the glycan linked at Asn-197 is affected, resulting in both Fuc residues (white) being in very close proximity to each other with resultant H-bond formations: Fuc-181 O2—O4 Fuc-197 (2.87 Å) and Fuc-181 O3—O4 Fuc-197 (3.19 Å) (Color Plate 3A). Moreover, both Fuc residues, especially that on the glycan at the Asn-197 site, are surrounded by a variety of residues

**Table 1. Mutant and Wild-Type *mPrP* (124–231) With or Without the N-glycan Showing Residues involved in H-bonding and Hydrophobic Interaction**

Mutation site	No. H-bonds	H-bond coordinates and length (Å)	Nonligand residues involved in hydrophobic contact of fixed residues
Asp-178-Asn PDB1ag2 data	4	Asp-178 OD1–NH1 Arg-164 (2.71) Asp-178 OD2–OH Tyr-128 (2.57) Asp-178 O–N Ile-182 (2.92) Asp-178 N–O Phe-175 (3.03)	a
Mutant-MD No glycan	2	Asn-178 ND2–O Gly-127 (2.91) Asn-178 N–O Asn-174 (2.86)	a
Glycan	3	Asn-178 OD1–NE Arg-164 (2.85) Asn-178 ND2–O Tyr-162 (2.82) Asn-178 O–N Ile-182 (3.29)	Tyr-128, first GlcNAc at Asn-181
Wild-type-MD No glycan	6	Asp-178 OD1–NE Arg-164 (2.97) Asp-178 OD1–NH2 Arg-164 (2.81) Asp-178 OD1–OH Tyr-128 (2.81) Asp-178 OD2–ND1 His-177 (2.83) Asp-178 N–O Phe-175 (3.02) Asp-178 O–N Ile-182 (2.92)	a
Glycan	6	Asp-178 OD1–NE Arg-164 (2.91) Asp-178 OD1–NH2 Arg-164 (2.78) Asp-178 OD1–OH Tyr-128 (2.79) Asp-178 OD2–ND1 His-177 (2.86) Asp-178 O–N Ile-182 (2.91) Asp-178 O–N Asn-181 (2.98)	a
Thr-183-Ala PDB1ag2 data	3	Thr-183 N–O Cys-179 (2.80) Thr-183 OG1–N Tyr-162 (3.10) Thr-183 O–N His-187 (2.82)	Val-161, Val-210
Mutant-MD No glycan	1	Ala-184 O–N His-187 (2.95)	Cys-179, Tyr-162
Glycan	1	Ala-183 N–O Cys-179 (2.91)	Val-210, Tyr-162
Wild type-MD No glycan	3	Thr-183 N–O Cys-179 (3.00) Thr-183 OG1–O Cys-179 (2.84) Thr-183 O–N His-187 (3.14)	Val-210
Glycan	4	Thr-183 N–O Cys-179 (2.84) Thr-183 OG1–O Cys-179 (2.78) Thr-183 O–N Thr-188 (3.05) Thr-183 O–N His-187 (2.92)	Tyr-162
Phe-198-Ser PDB1ag2 data	0	No H-bond contacts	Asp-202, Tyr-157 Glu-196, Arg-156 Met-206, His-187
Mutant-MD No glycan	0	No H-bond contacts	a
Glycan	0	No H-bond contacts	Val-203
Wild-type-MD No glycan	1	Phe-198 N–O Glu-196 (2.85)	Thr-191, Thr-188, Val-203, Met-206
Glycan	0	No H-bond contacts	Asp-202, Glu-196, Thr-188, Met-206, Arg-156, Tyr-157

**Table 1.** (Continued)

Mutation site	No. H-bonds	H-bond coordinates and length (Å)	Nonligand residues involved in hydrophobic contact of fixed residues
Glu-200-Lys			
PDB1ag2 data	1	Glu-200 O–N Lys-204 (2.87)	a
Mutant–MD			
No glycan	1	Lys-200 O–N Val-203 (3.02)	a
Glycan	1	Lys-200 O–N Lys-204 (2.90)	a
Wild-type–MD			
No glycan	3	Glu-200 O–N Lys-204 (3.11) Glu-200 OE1–NZ Lys-204 (2.90) Glu-200 OE2–OG1 Thr-201 (2.92)	a
Glycan	3	Gly-200 O–N Lys-204 (3.07) Gly-200 OE1–NZ Lys-204 (2.82) Gly-200 OE2–NZ Lys-204 (2.80)	a
Gln-217-Arg			
PDB1ag2 data	2	Gln-217 NE2–O Ala-133 (2.88) Gln-217 N–O Met-213 (2.89)	Tyr-163
Mutant–MD			
No glycan	7	Arg-217 NH1–O Ala-133 (2.84) Arg-217 NH1–O Gly-131 (3.19) Arg-217 NH2–O Thr-216 (2.92) Arg-217 NH2–OG Ser-135 (2.81) Arg-217 NE–O Thr-216 (2.99) Arg-217 NE–O Met-213 (2.94) Arg-217 N–O Val-215 (2.84)	Tyr-163, Val-161
Glycan	3	Arg-217 NH2–OG Ser-132 (2.89) Arg-217 O–N Gln-219 (2.97) Arg-217 N–O Val-215 (2.86)	Met-134, Gly-131, Ala-133
Wild-type–MD			
No glycan	4	Gln-217 N–O Val-215 (2.82) Gln-217 NE2–O Ser-132 (3.32) Gln-217 OE1–N Ser-132 (2.92) Gln-217 OE1–OG Ser-132 (2.92)	Tyr-163, Val-161, Gly-131
Glycan	3	Gln-217 N–O Met-213 (2.81) Gln-217 NE2–O Ser-132 (3.01) Gln-217 OE1–N Ser-132 (2.99)	Tyr-163, Gly-131

a = No hydrophobic contacts with nonligand residues; MD = molecular dynamics simulation; PDB1ag2 = original PDB data of *mPrP*<sup>C</sup> (124–226) (see text for details).

involved in H-bond and hydrophobic interactions (Table 1), and there is a decrease of  $\alpha$ -helix content. The proximity of the two glycosylation sites may influence their occupancy, which is consistent with the SDS-PAGE analysis. Conversely, the distances of both glycans shown in the wild-type (Color Plate 3B) are spaced far apart, with little or no influence on local protein conformation.

**Asp-178-Asn** Riek et al.<sup>11</sup> suggest that the amino acid replacement of Asp-178 to Asn removes the salt bridge between the conserved residues Asp-178–Arg-164 that hold the  $\beta$ -sheet against helix 2, thus causing reduced thermodynamic stability of the protein. In the modeling of the nonglycosylated mutant, two new H-bonds are present from Gly-127 and Asn-174 (Table 1). The amino acid replacement causes the abolition of H-bonds found in the two  $\beta$ -sheets from Arg-164 and

Tyr-128 to the side chain of Asp-178, as present in the PDB1ag2 data. Also, Asp-178 is expressed on an external surface of the protein and is next to the first residue of the disulfide bond (Cys-179), which may have too little flexibility for modeling studies. In the mutant containing glycan (Table 1), two of the original four H-bonds from Arg-164 and Ile-182 are present, as shown in the PDB1ag2 data. Interestingly, GlcNAc linked to Asn-181 forms hydrophobic interactions with the mutant residue of Asn-178. For both wild-types containing glycan and nonglycan, two extra residues of a total of six are involved in H-bond contacts when compared to the PDB1ag2 data. The results of SDS-PAGE (Figure 2) show minor changes in glycosylation occupancy. In both wild-types and mutants, the residue with Met-129 polymorphism is present. Table 1 shows that Asn-178 is in close proximity to

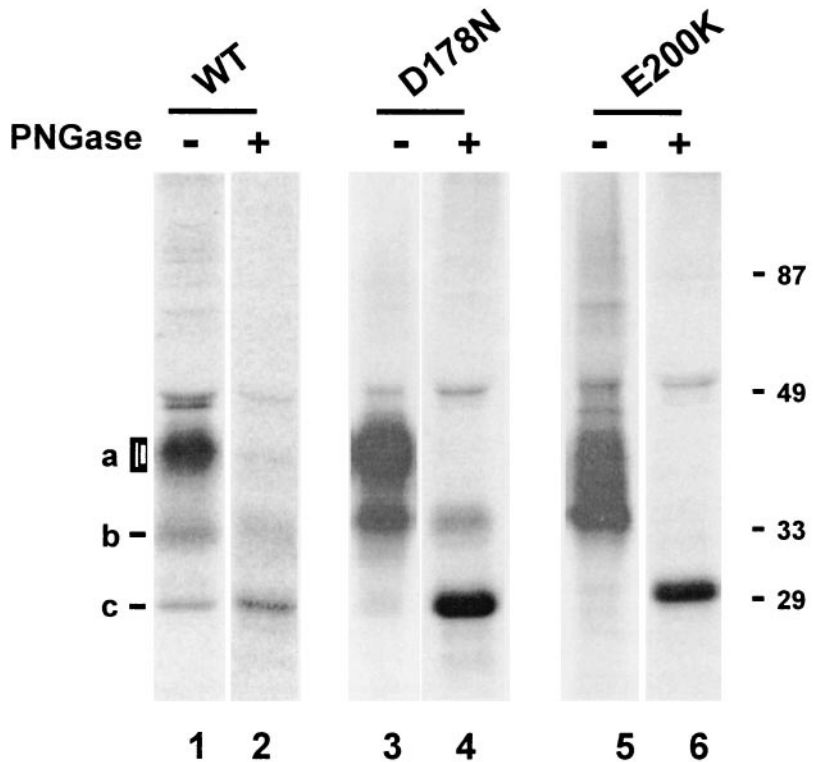


**Figure 2.** SDS-PAGE showing the glycosylation pattern of the wild-type (WT) and two mutants D178N and E200K.

Gly-127 in the mutant in the absence of glycosylation only, whereas Asp-178 is close to Tyr-128 in both glycosylated and nonglycosylated forms.

**Thr-183-Ala** Observations on the amino acid replacement, Thr-183-Ala without glycan (Table 1), agrees with the findings of Riek et al.<sup>11</sup> indicating that the H-bonding in which both Cys-179 and Tyr-162 were involved was abolished by this mutation. The result is only one new H-bond formation, Ala-183 O-N His-187, from the original three H-bonds. The new bond formation may reduce the stability of this protein variant as Thr-183-Ala is located in the center of helix 2. Also, the resultant hydrophobic contacts of this mutant are changed from Val-161 and Val-210 (of the original PDB1ag2 data) to Cys-179 and Tyr-162. Comparing the mutant (which would not be glycosylated *in vivo*) with the wild-type containing glycan (Table 1), the same result occurs: two H-bonds are abolished leaving only one H-bond present. However, instead of His-187, the residue Cys-179 is H-bonded to Ala-183. The hydrophobic contact to fixed residues is similar to the PDB1ag2 data in which residues Val-210 and Tyr-162 are present. In the nonglycosylated wild-type after MD, three H-bonds are conserved as in the original PDB1ag2 data. However, Tyr-162 H-bond is not present (Table 1) but is replaced by H-bonds Thr-183 OH<sup>β</sup>-O Cys-179 and Thr-183 N-O Cys-179. In the wild-type containing glycan, the residues involved in H-bonding are the same as the nonglycan wild-type, but with an extra H-bond, Thr-183 O-N Thr-188. Studies by Nitriini et al.<sup>27</sup> indicated that a mutation homologous to Thr-183-Ala is the cause of inherited spongiform encephalopathy in humans.

**Gln-217-Arg** The original PDB1ag2 data indicate that a long-range H-bond to the carbonyl oxygen of Ala-133 is present that stabilizes a distinct position of the loop between

the first β-strand and helix 1 relative to the hydrophobic core. Riek et al.<sup>11</sup> suggested that replacement of Gln-217 to Arg, which introduces a positive charge to this uncharged region, would lead to unsatisfactory H-bond geometry of the carbonyl oxygen of Ala-133 with the Arg side chain. The mutation site Gln-217-Arg is at the end of helix 3 on a sort of helical bend, and residues 209-224 seem to cover this helix. Over the top of Gln-217 is the extended helix 128-137, under which residues 158-164 also lie alongside the helix. These sequences were fixed in the modeling that gave five extra H-bonds for the mutant containing nonglycan (Table 1), in addition to the two residues that are involved in H-bonding (Ala-133 and Met-213) present in the PDB1ag2 data. Three new H-bonds (from Ser-132, Gln-219 to Val-215) are present in the mutant containing glycan. Residue Ala-133, in addition to two others (Met-134 and Gly-131), is now involved with hydrophobic interaction to fixed residues. For both wild-types containing glycan and non-glycan, Ala-133 is moved by one residue and replaced by Ser-132 as the dominant residue involved in H-bonding.

## DISCUSSION

In this study, modeling of glycosylated PrP in both mutant and wild-type forms with and without the core trisaccharide region [GlcNAc $\beta$ 1-4(Fuc $\alpha$ 1-6)GlcNAc $\beta$ 1-] was performed to demonstrate the effect of glycosylation on protein conformation. These studies demonstrated that, by using MD, we could recreate experimental models produced by Riek et al.<sup>11</sup> by predicting protein stability due to changes in internal H-bond and hydrophobic interactions of mutants. In addition, the modeling of the mutant Glu-200-Lys went further than the NMR experiments to explain the cell expression data of altered glycosylation. For further studies on glycosylation structure and func-

tion, molecular modeling will be useful to predict possible interactions of glycosylated PrP mutants with endogenous ligands such as glycosaminoglycans.

N-linked glycosylation of PrP is likely to be functionally and physiologically important in prion biology. Thus, glycosylation represents an important aspect of PrP conformation as demonstrated by visualization of the mutants in this study. Studies show that the presence of modified glycosylation or different glycan structures (glycoforms) may be a useful marker of various prion strains.<sup>3,6,8</sup> In addition, mutational activation of one of the two consensus sites for N-linked glycosylation may lead to inherited spongiform encephalopathy.<sup>27</sup> Stimson et al.<sup>18</sup> characterized various glycoforms present at positions Asn-180 and Asn-196 in murine prion protein (equivalent to human Asn-181 and Asn-197, respectively). The authors demonstrated that the Le<sup>x</sup> trisaccharide (present in our initial model) is the major nonreducing structure in Asn-180, whereas significant amounts of both Le<sup>x</sup> and sialyl Le<sup>x</sup> epitopes are observed at Asn-196. The presence of Le<sup>x</sup> and sialyl Le<sup>x</sup> epitopes on mPrP<sup>Sc</sup> may be important in the physiological functions of PrP<sup>C</sup> or lead to the pathophysiology of PrP<sup>Sc</sup>.<sup>18</sup>

In amyloidosis, a pathogenic process occurs in which normally soluble proteins aggregate to form insoluble amyloid fibrils. Associated with amyloid deposits are the amyloid P component and glycosaminoglycans (GAGs).<sup>28</sup> Moreover, the presence of glycosylation in some amyloidogenic proteins may either predispose to fibril formation<sup>29</sup> or inhibit fibril formation as suggested for PrP.<sup>5</sup> Studies on pentosan sulfate (PS), a synthetic polyanionic glycan that is structurally related to GAGs, showed a direct interaction with PrP, which alters protein trafficking. It is suggested that PS prevents prion accumulation by interfering or competing with the interaction of PrP<sup>C</sup> precursor with GAGs, and that GAGs are likely to play an important role in the cellular metabolism of both PrP<sup>Sc</sup> and PrP<sup>C</sup>.<sup>30–32</sup> The proposal that PrP interacts with cellular GAGs is suggested by studies demonstrating that amyloid plaques in scrapie-infected brain often contain sulfated proteoglycans.<sup>33</sup> Moreover, it is possible that the density of sulfation and its relative molecular size may be one of several factors influencing anti-PrP<sup>Sc</sup> activity by sulfated glycans. However, direct evidence for the existence of GAG-related binding sites on cells for either PrP<sup>C</sup> and PrP<sup>Sc</sup> is still lacking. Possibly though, the N-terminal of PrP may be a potential ligand for binding of GAG or related glycans (R. Morris, UDMS, Guys Hospital Medical School, personal communication).

To further support the effect of glycosylation on prion formation, Lehmann and Harris<sup>5</sup> studied the role of N-glycans in determining the properties of PrP in which glycosylation has been blocked by replacement of Thr-183 and Thr-199 to Ala at one or both of the AsnXaaThr/Ser consensus sites. The authors suggest that N-linked glycans are not necessary for normal biosynthetic trafficking of PrP. However, results indicate that PrP proteins mutated at Thr-183 alone or at both Thr-183 and Thr-199 fail to reach the cell surface after synthesis, and that those mutated at Thr-199 can be detected on the plasma membrane. Therefore, one residue rather than the other is important in protein trafficking. Localization of those molecules that fail to reach the plasma membrane remains to be determined. It is likely to be proximal to the mid-Golgi stack because the mutant protein remained sensitive to Endo H.<sup>34</sup> DeArmond et al.<sup>35</sup> suggested that Asn-linked glycosylation would affect the affinity of PrP<sup>C</sup> for a particular conformer of PrP<sup>Sc</sup>, thereby

determining the rate of nascent PrP<sup>Sc</sup> formation and the specific patterns of PrP<sup>Sc</sup> formation. Petersen et al.<sup>36</sup> also studied an Asp-178-Asn mutant that causes protein instability and misfolding. They found that this mutant was retained and degraded in a pre-Golgi compartment. Studies have demonstrated that PrP<sup>Sc</sup> synthesized in infected cells in the presence of tunicamycin, which blocks glycosylation, is enriched in higher molecular weight glycoforms,<sup>37,38</sup> and PrP<sup>Sc</sup> is produced more rapidly in scrapie-infected neuroblastoma cells treated with tunicamycin.<sup>39</sup>

It should be noted that PrP<sup>Sc</sup> strains can be distinguished by different glycosylation patterns after proteinase K digestion. These patterns may be caused by selective degradation of specific glycoforms<sup>36</sup> or enzymatic removal or modification of glycan chains. Thus, it is possible that the presence of subtle differences in the structure and composition of oligosaccharide chains can influence the properties of the protein and characterize different PrP<sup>Sc</sup> strains. Importantly, visualization of the mutants can demonstrate how glycosylation correlates with the conformation of the PrP polypeptide. One can predict how each oligosaccharide chain is added to the PrP mutant and acquires various characteristics due to generation of possible glycoform diversity and the effect of the glycan itself.

## ACKNOWLEDGMENTS

This work is supported by Grant PL976055 from the EU-BIOTECH Research Grant and the Medical Research Council (MRC). SDS-PAGE analysis was derived from experiments carried out in the laboratory of Dr. D. Harris, Department of Cell Biology & Physiology, Washington University School of Medicine, St. Louis, Missouri, USA.

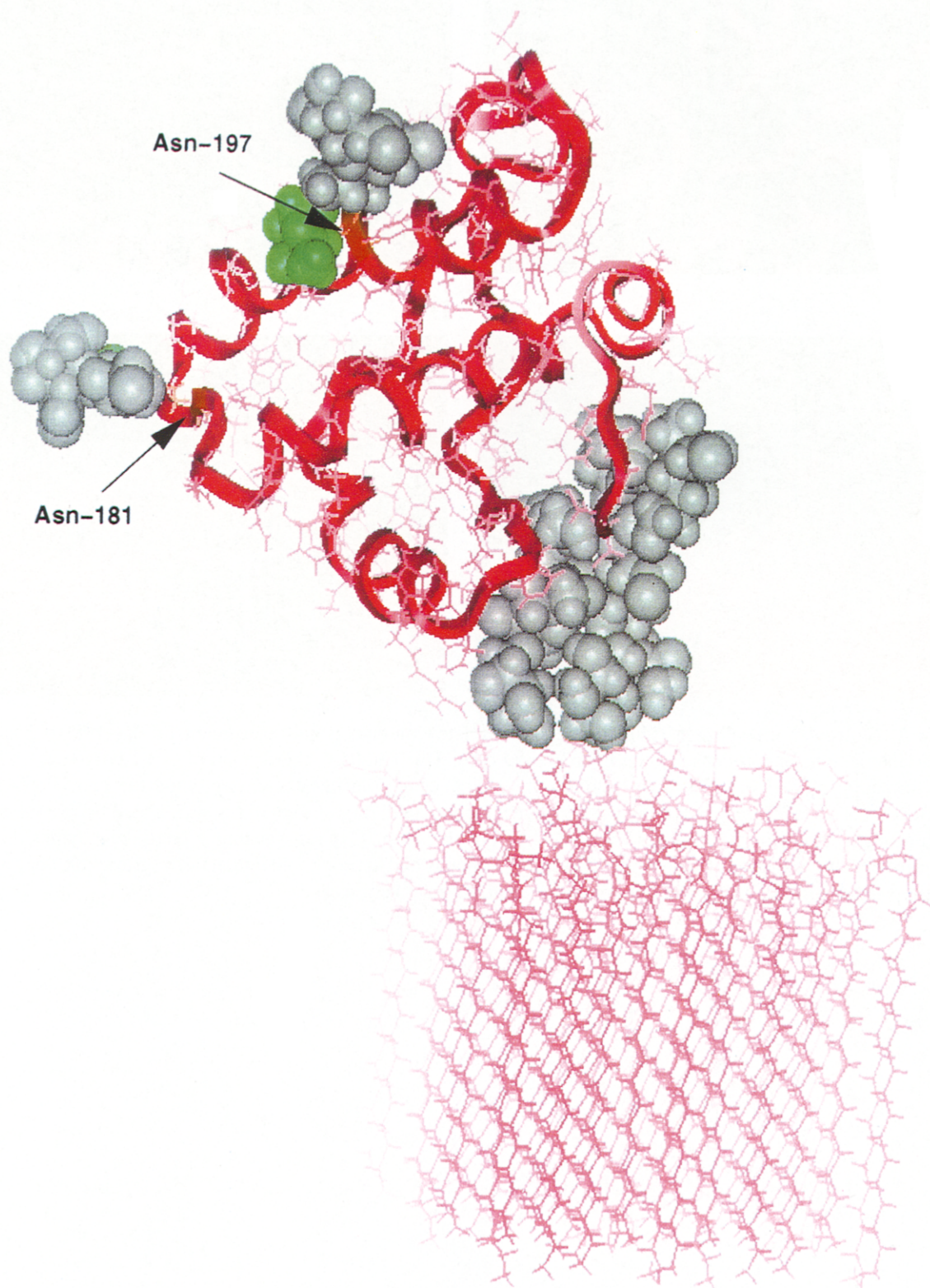
## REFERENCES

- 1 Prusiner, S.B., Bolton, D.C., Groth, D.F., Bowman, K.A., Cochran, S.P., and McKinley, M.P. Further purification and characterization of scrapie prions. *Biochemistry* 1982, **21**, 6942–6950
- 2 Haraguchi, T., Fisher, S., Olofsson, S., Endo, T., Groth, D., Tarentino, A., Borchelt, D.R., Teplow, D., Hood, L., Burlingame, A., Lycke, E., Kobata, A., and Prusiner, S.B. Asparagine-linked glycosylation of the scrapie and cellular prion proteins. *Arch. Biochem. Biophys.* 1989, **274**, 1–13
- 3 Stahl, N., Baldwin, M.A., Teplow, D.B., Hood, L., Gibson, G.W., Burlingame, A.L., and Prusiner, S.B. Structural studies of the scrapie protein using mass spectrometry and amino acid sequencing. *Biochemistry* 1993, **32**, 1991–2002
- 4 Cohen, F.E., Pan, K., Huang, Z., Baldwin, M., Fletterick, R.J., and Prusiner, S.B. Structural clues to prion replication. *Science* 1994, **264**, 530–531
- 5 Lehmann, S., and Harris, D.A. Blockade of glycosylation promotes acquisition of scrapie-like properties by the prion protein in cultured cells. *J. Biol. Chem.* 1997, **272**, 21479–21487
- 6 Collinge, J., Sidle, K.C.L., Meads, J., Ironside, J., and Hill, A.F. Molecular analysis of prion strain variation and the aetiology of “new variant” CJD. *Nature* 1996, **383**, 685–690
- 7 Parchi, P., Castellani, R., Capellari, S., Ghetti, B., Young, K., Chen, S.G., Farlow, M., Dickson, D.W.,

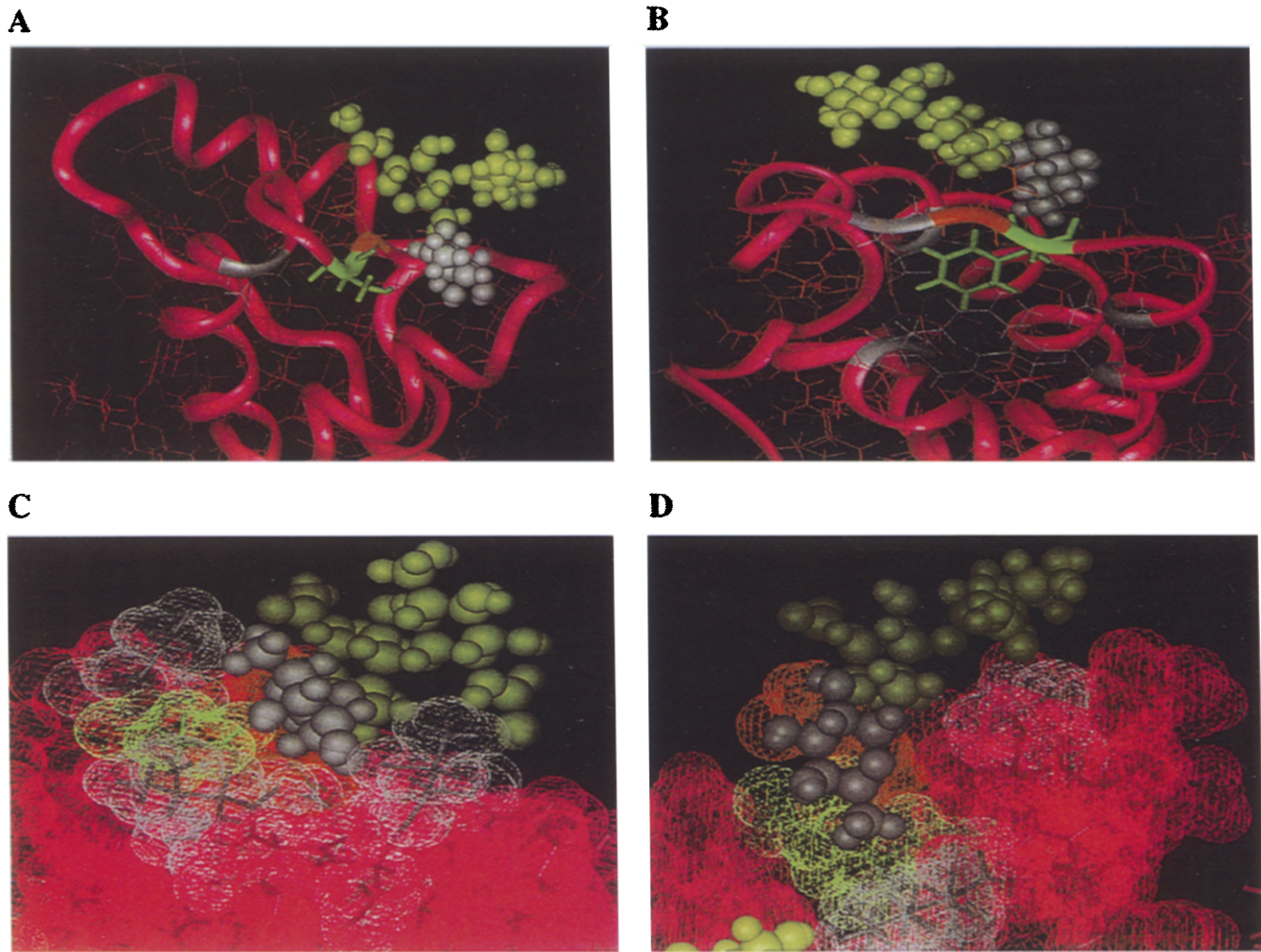
- Sima, A.A.F., Trojanowski, J.Q., Petersen, R.B., and Gambetti, P. Molecular basis of phenotypic variability in sporadic Creutzfeldt-Jakob disease. *Ann. Neurol.* 1996, **39**, 767–778
- 8 Monari, L., Chen, S.G., Brown, P., Parchi, P., Petersen, R.B., Mikol, J., Gray, F., Cortelli, P., Montagna, P., Ghetti, B., Goldfarb, L., Gajdusek, D.C., Lugaresi, E., Gambetti, P., and Autilio-Gambetti, L. Fatal familial insomnia and familial Creutzfeldt-Jakob disease: Different prion proteins determined by DNA polymorphism. *Proc. Natl. Acad. Sci. U. S. A.* 1994, **91**, 2839–2842
- 9 Riek, R., Hornemann, S., Wider, G., Billeter, M., Glockshuber, R., and Wüthrich, K. NMR characterization of the full-length recombinant murine prion protein, mPrP (23–231). *FEBS Lett.* 1997, **413**, 282–288
- 10 Riek, R., Hornemann, S., Wider, G., Billeter, M., Glockshuber, R., and Wüthrich, K. NMR structure of the mouse prion protein domain, PrP (121–321). *Nature* 1996, **382**, 180–182
- 11 Riek, R., Wider, G., Billeter, M., Hornemann, S., Glockshuber, R., and Wüthrich, K. Prion protein NMR structure and familial spongiform encephalopathies. *Proc. Natl. Acad. Sci. U. S. A.* 1998, **95**, 11667–11672
- 12 Prusiner, S.B. Molecular biology and genetics of prion diseases. *Philos. Trans. R. Soc. Lond. B Biol. Sci.* 1994, **343**, 447–463
- 13 Harrison, P.M., Bamforth, P., Daggett, V., Prusiner, S.B., and Cohen, F.E. The prion folding problem. *Curr. Opin. Struct. Biol.* 1997, **7**, 53–59
- 14 Goldfarb, L.G., Petersen, R.B., Tabaton, M., Brown, P., LeBlanc, A.C., Montagna, P., Cortelli, P., Julien, J., Vital, C., Pendelbury, W.W., Haltia, M., Wills, P.R., Hauw, J.J., McKeever, P.E., Monari, L., Schrank, B., Swerdlow, G.D., Autilio-Gambetti, L., Gajdusek, D.C., Lugaresi, E., and Gambetti, P. Fatal familial insomnia and familial Creutzfeldt-Jakob disease: Disease phenotype determined by a DNA polymorphism. *Science* 1992, **258**, 806–808
- 15 Palmer, M.S., Dryden, A.J., Hughes, J.T., and Collinge, J. Homozygous prion protein genotype predisposes to sporadic Creutzfeldt-Jakob disease. *Nature* 1991, **352**, 340–342
- 16 Tateishi, J., and Kitamoto, T. Developments in diagnosis for prion diseases. *Br. Med. Bull.* 1993, **49**, 971–979
- 17 Weissmann, C. Prion diseases. Yielding under the strain. *Nature* 1995, **375**, 628–629
- 18 Stimson, E., Hope, J., Chong, A., and Burlingame, A.L. Site-specific characterization of the N-linked glycans of murine prion protein by high-performance liquid chromatography/electrospray mass spectrometry and exoglycosidase. *Biochemistry* 1999, **38**, 4885–4895
- 19 Renouf, D.V., and Hounsell, E.F. Conformational studies of the backbone (poly-N-acetyllactosamine) and the core region sequences of O-linked carbohydrate chains. *J. Biol. Macromol.* 1993, **15**, 37–42
- 20 Imbert, A., Delage, M.-M., Bourne, Y., Cambillau, C., and Perez, J. Data bank three-dimensional structures of disaccharides. Part II. N-acetyllactoseamine type N-glycans. Comparison with the crystal structure of a bi-antennary octasaccharide. *Glyconjug. J.* 1991, **8**, 456–483
- 21 Imbert, A., Gerber, S., Tran, V., and Perez, J. Data bank of three-dimensional structures of disaccharides, a tool to build 3-D structures of oligosaccharides. Part I. Oligo mannose type N-glycans. *Glyconjug. J.* 1990, **7**, 27–54
- 22 Wallace, A.C., Laskowski, R.A., and Thornton, J.M. LIGPLOT: A program to generate schematic diagrams of protein-ligand interactions. *Prot. Eng.* 1993, **8**, 127–134
- 23 Lehmann, S., and Harris, D.A. Mutant and infectious prion proteins display common biochemical properties in cultured cells. *J. Biol. Chem.* 1996, **271**, 1633–1637
- 24 Lehmann, S., and Harris, D.A. Two mutant prion proteins expressed in cultured cells acquire biochemical properties reminiscent of the scrapie isoform. *Proc. Natl. Acad. Sci. U. S. A.* 1996, **93**, 5610–5614
- 25 Lehmann, S., and Harris, D.A. A mutant prion protein displays an aberrant membrane association when expressed in cultured cells. *J. Biol. Chem.* 1995, **270**, 24589–24597
- 26 Gabizon, R., Rosenman, H., Meiner, Z., Kahana, I., Kahana, E., Shugart, Y., Ott, J., and Prusiner, S.B. Mutation in codon 200 and polymorphism in codon 129 of the prion protein gene in Libyan Jews with Creutzfeld-Jakob disease. *Philos. Trans. R. Soc. Lond. B Biol. Sci.* 1994, **343**, 385–390
- 27 Nitrini, R., Rosenberg, S., Passos-Bueno, M.R., da Silva, L.S., Iughetti, P., Papadopoulos, M., Carrilho, P.M., Caramelli, P., Albrecht, S., Zatz, M., and LeBlanc, A. Familial spongiform encephalopathy associated with a novel prion protein gene mutation. *Ann. Neurol.* 1997, **42**, 138–146
- 28 Stenstad, T., Magnus, J.H., Syse, K., and Husby, G. On the association between amyloid fibrils and glycosaminoglycans: Possible interactive role of  $\text{Ca}^{2+}$  and amyloid fibrils: Immunoglobulin light chains. *Biochemistry* 1993, **34**, 10697–10702
- 29 Wang, J.-Z., Grundke-Iqbali, I., and Iqbal, K. Glycosylation of microtubule-associated protein tau: An abnormal posttranslational modification in Alzheimer's disease. *Nat. Med.* 1996, **2**, 871–875
- 30 Shyng, S.L., Lehmann, S., Moulder, K.L., and Harris, D.A. Sulfated glycans stimulate endocytosis of the cellular isoform of the prion protein, PrP<sup>C</sup>, in cultured cells. *J. Biol. Chem.* 1995, **270**, 30221–30229
- 31 Priola, S.A., and Caughey, B. Inhibition of scrapie-associated PrP accumulation. Probing the role of glycosaminoglycans in amyloidogenesis. *Mol. Neurobiol.* 1994, **8**, 113–120
- 32 Caughey, B., and Raymond, G.J. Sulfated polyanion inhibition of scrapie-associated PrP accumulation in cultured cells. *J. Virol.* 1993, **67**, 643–650
- 33 Snow, A.D., Wight, T.N., Nochlin, D., Koike, Y., Kimata, K., DeArmond, S.J., and Prusiner, S.B. Immunolocalization of heparan sulfate proteoglycans to the prion protein amyloid plaques of Gerstmann-Straussler syndrome, Creutzfeldt-Jakob disease and scrapie. *Lab. Invest.* 1990, **63**, 601–611
- 34 Rogers, M., Taraboulos, A., Scott, M., Groth, D., and Prusiner, S.B. Intracellular accumulation of the cellular prion protein after mutagenesis of its Asn-linked glycosylation sites. *Glycobiology* 1990, **1**, 101–109
- 35 DeArmond, S.J., Sanchez, H., Yehiely, F., Qiu, Y., Ninchak-Casey, A., Daggett, V., Camerino, A.P., Cayetano, J., Rogers, M., Groth, D., Torchia, M., Tremblay, P., Scott, M.R., Cohen, F.E., and Prusiner, S.B. Selective

- neuronal targeting in prion disease. *Neuron*. 1997, **19**, 1337–1348
- 36 Petersen, R.B., Parchi, P., Richardson, S.L., Urig, C.B., and Gambetti, P. Effect of the D178N mutation and the codon 129 polymorphism of the metabolism of the prion protein. *J. Biol. Chem.* 1996, **271**, 12661–12668
- 37 Tatzelt, J., Prusiner, S.B., and Welch, W.J. Chemical chaperons interfere with the formation of scrapie prion protein. *EMBO J.* 1996, **15**, 6363–6373
- 38 Caughey, B., and Raymond, G.J. The scrapie-associated form of PrP is made from a cell surface precursor that is both protease- and phospholipase-sensitive. *J. Biol. Chem.* 1991, **266**, 18217–18223
- 39 Taraboulous, A., Rogers, M., Borchelt, D.R., McKinley, M.P., Scott, M., Serban, D., and Prusiner, S.B. Acquisition of protease resistance of prion proteins in scrapie-infected cells does not require asparagine-linked glycosylation. *Proc. Natl. Acad. Sci. U. S. A.* 1990, **87**, 8262–8266

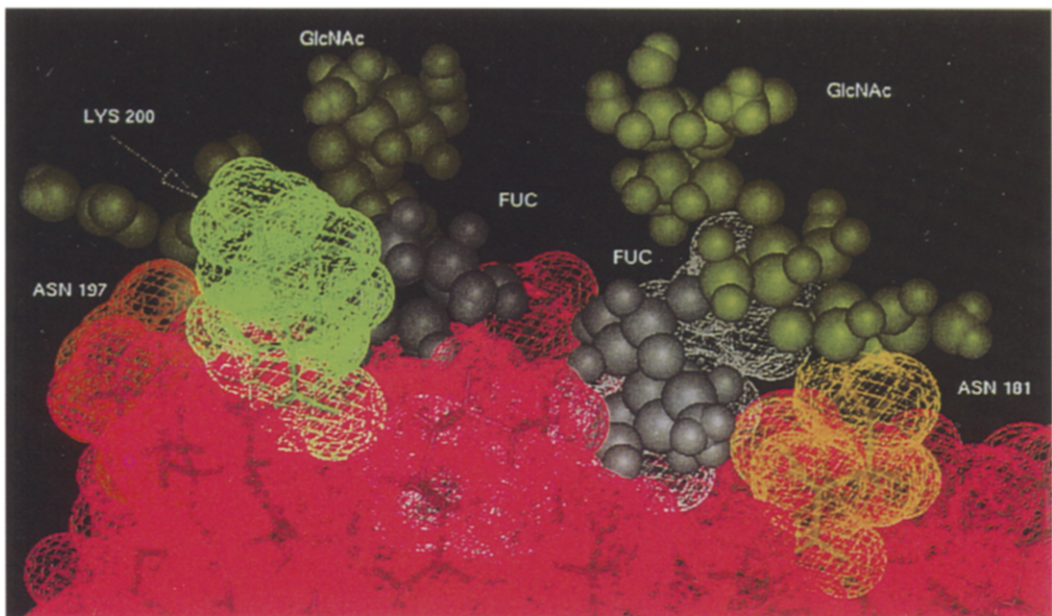
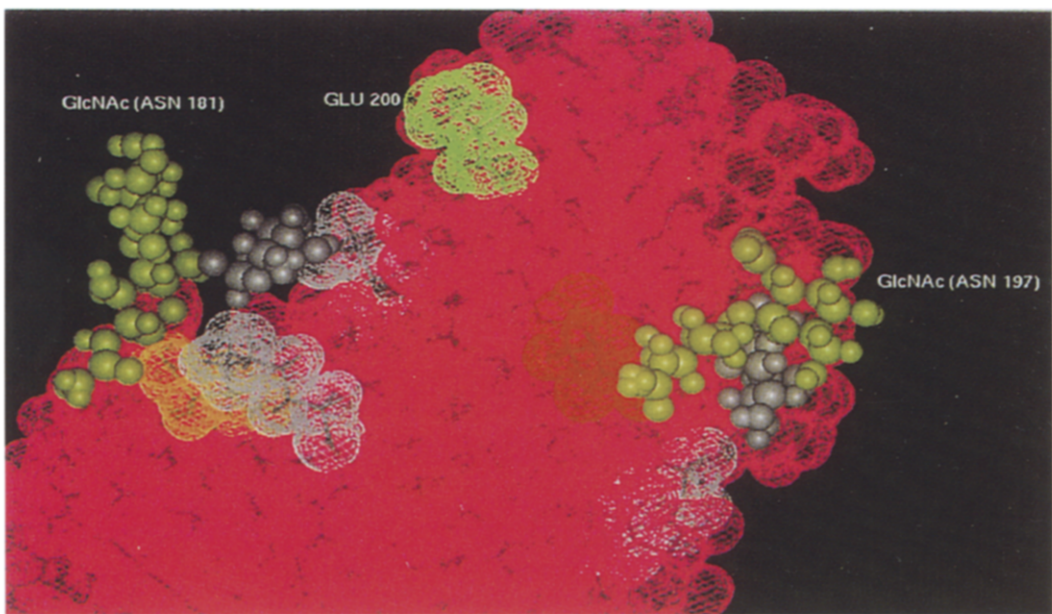
**Glycosylation of prions and its effects on protein conformation relevant to amino acid mutations**



Color Plate 1. Wild-type prion modeled from the protein NMR coordinates of Riek et al.<sup>11</sup> showing the added trisaccharides at positions Asn-181 and Asn-197. The glycan of the GPI anchor (gray) is shown attached to the lipid membrane.



Color Plate 2. Molecular modeling of Phe-198-Ser glycosylated mutant. (A) Replacement of Phe-198 to Ser abolishes hydrophobic interactions and collapse of the hydrophobic core. This results in the formation of a cavity space with altered glycan conformation at Asn-197. The Fuc residue (white) is "nesting" inside this cavity while the two GlcNAc residues (yellow) affect local surface structure. (B) In the wild-type, the aromatic ring of Phe-198 is surrounded by residues at various positions, forming hydrophobic interactions within the hydrophobic core. (C) Closer examination of the mutant shows that the glycan is surrounded by a variety of independently formed H-bonds and hydrophobic interactions (gray). (D) For comparison, in the wild-type, the influence of glycan on protein structure is relatively weak.

**A****B**

Color Plate 3. Molecular modeling of Glu-200-Lys mutant. (A) In the mutant, both Fuc residues (white) linked to the GlcNAc (yellow) at positions Asn-181 and Asn-197 are in very close proximity to each other, resulting in H-bonding formation. (B) Conversely, the distances of both glycans shown in the wild-type are spaced far apart, with little or no influence on local protein conformation.